This is a repository copy of *Tool path generation for single point incremental forming using intelligent sequencing and multi-step mesh morphing techniques*.

White Rose Research Online URL for this paper:
http://eprints.whiterose.ac.uk/97142/

Version: Accepted Version

Tool path Generation for Single Point Incremental Forming using Intelligent Sequencing and Multi-step Mesh Morphing Techniques

Amar Kumar Behera[a], Bert Lauwers[b], Joost R. Duflou[c]

Katholieke Universiteit Leuven, Department of Mechanical Engineering, Celestijnenlaan 300B, B-3001 Leuven, Belgium

[a]amarkumar.behera@cib.kuleuven.be, [b]bert.lauwers@mech.kuleuven.be, [c]joost.duflou@mech.kuleuven.be

Keywords: Incremental Forming, mesh morphing, intelligent sequencing, optimal tool paths, STL

Abstract. A new methodology of generating optimized tool paths for incremental sheet forming is proposed in this work. The objective is to make parts with improved accuracy. To enable this, a systematic, automated technique of creating intermediate shapes using a morph mapping strategy is developed. This strategy is based on starting with a shape different from the final shape, available as a triangulated STL model, and using step-wise incremental deformation to the original mesh to arrive at the final part shape. Further, optimized tool path generation requires intelligent sequencing of partial tool paths that may be applied specifically to certain features on the part. The sequencing procedure is discussed next and case studies showing the application of the integrated technique are illustrated. The accuracy of the formed parts significantly improves using this integrated technique. The maximum deviations are brought down to less than 1 mm, while average absolute deviations of less than 0.5 mm are recorded.

Introduction

In recent years, asymmetric incremental sheet forming (AISF) has emerged as a flexible, dieless forming process for sheet metal parts, which overcomes some of the limitations of traditional sheet forming [1]. As different research groups worldwide have tried to make this process industrially viable, several process variants have emerged. These include using a single point of contact known as Single Point Incremental Forming (SPIF) [1-2], using two points of contact or Two Point Incremental Forming (TPIF) [1,3], using a partial die [1], and using a full die [1]. Each process variant comes with a set of limitations. Of these variants, SPIF offers the greatest flexibility in terms of part manufacture, as the process can be performed dielessly using a single tool on a setup such as a milling machine or a robot which is fed with a computer generated tool path conforming to the final part shape (see schematic in Fig.1). The other variants requires additional constraints such as synchronization of two tools, partial or full die manufacture etc.

However, the manufacture of complex 3D parts using Single Point Incremental Forming (SPIF) is often challenging due to the simultaneous requirements of high forming angles and accuracy specifications to maintain part functionality as required by the customer. In particular, incremental forming has been carried out on a wide range of materials including polymers [4-5], many of which have low forming limits, typically defined by a maximum wall angle at which no failure occurs. In addition, several efforts have been made to improve the accuracy of parts [6-9]. For instance, Verbert et al. developed a feature based approach, where the behavior of individual features such as planes, ruled, freeform and ribs is taken into account to manufacture parts with high accuracy [7]. In this approach, the triangulated CAD model of a part available in STL file format is used to detect features. For individual features, the vertices are translated based on actual deviations of a test part or models of anticipated deviations to create a compensated CAD model. Tool paths are generated on these compensated models and produce more accurate parts compared to parts made with tool paths on the original CAD or uncompensated model (Fig. 2).

The feature based approach of Verbert is illustrated only for simple feature behavior such as for planes well below the failure wall angle. Compensation strategies cannot be applied using this simple approach for parts close to failure. Behera et al. suggest the use of a mathematical compensation technique using Multivariate Adaptive Regression Splines (MARS) [6]. However, this technique is also not very well suited to parts close to the forming limit. Likewise, parts made using a multi-step approach can contribute to process window extension [10]. The use of a dynamic heat source has helped improve both formability and accuracy to a limited extent [11].
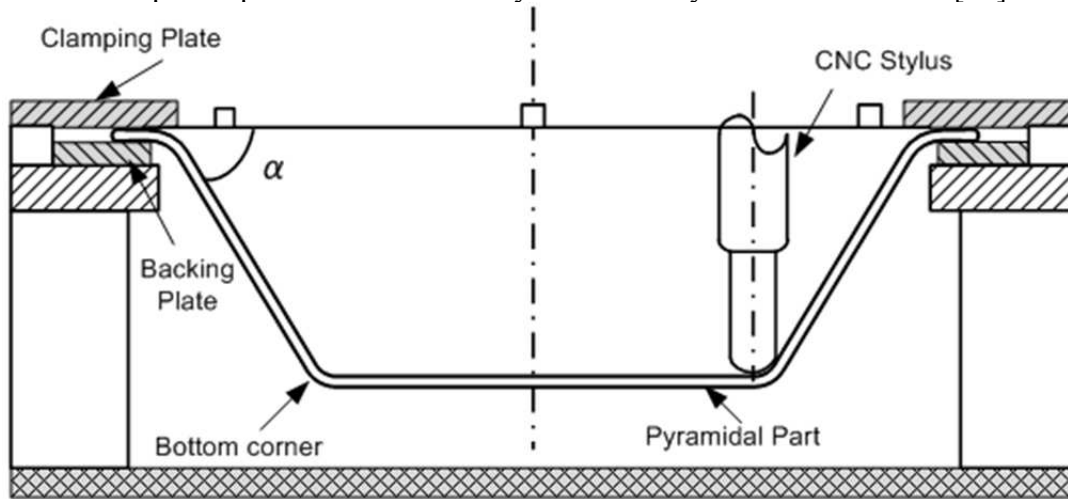
Fig.1. Schematic of a Single Point Incremental Forming set up
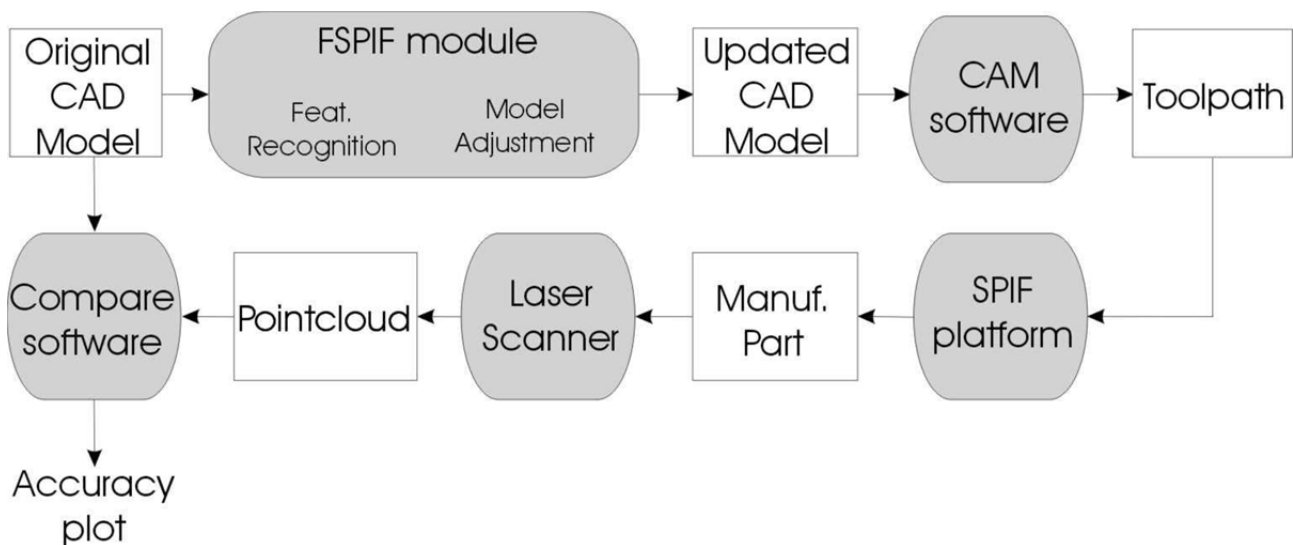
Fig.2. Feature-assisted Single Point Incremental Forming (FSPIF) schematic: a computer based FSPIF module is used to recognize features, adjust the CAD model of the part to be formed; the updated CAD model is used to generate a toolpath on the machine used for SPIF; the manufactured part is scanned with a laser to generate a point cloud which is compared with the original CAD to generate an accuracy plot.

Hence, despite these approaches, a need exists to develop tool path techniques that can help manufacture parts with both high forming angles and high accuracy. A need also exists to develop an automated and systematic procedure for multi-step part manufacture. In past work, the multi-step procedure is illustrated for simple ruled features such as cones [10] and cups [12], where the generation of intermediate shapes is evident as the final part has a constant slope or a well defined variation in the wall angles. But, no systematic procedure is present in literature for the generation

of intermediate shapes for parts with varying wall angles. Yet another issue is that the manufacture of truncated pyramidal shapes where the planar features are separated by rib features of high curvature and have forming limits beyond failure has hitherto not been demonstrated, as the conventional multi-step strategy fails for such parts.

Hence, in this research, an attempt was made to develop a mesh morphing based tool path generation strategy and integrate it with intelligent sequencing to make parts, especially containing high forming angles, with high accuracy. Case studies are presented to illustrate the successful implementation of the developed methodology.

Tool path generation requirements for incremental forming

The generation of optimized tool paths for incremental forming of high forming angle, high accuracy parts needs to be performed keeping in mind the following aspects: i) accuracy and forming behavior of high wall angle features ii) interactions between high wall angle features and other features in a part, and iii) offset distances between successive tool paths. These issues are discussed below.

   Behavior of high wall angle features. The forming of parts with high angles is typically done with a multi-step procedure, where the same geometry is made with a lower wall angle first and then increased in steps to the higher wall angle. Three different effects are observed in such forming techniques, viz.: i) high curvature areas such as ribs tend to fail first, in particular, if the tool path used is a contouring tool path with step down at the location of the ribs, ii) the final feature has, in general, a high accuracy for planar and positive curvature features (radius of curvature pointing into the part cavity) as compared to single pass tool paths for the same features due to reduction in spring back as a result of multiple processing, and iii) mild over forming effects may be observed in discrete locations.

   To illustrate these three effects, a set of cases which were performed are reported in Table 1. It can be seen here that the maximum deviation and average deviation for a truncated pyramid with wall angle 60° is significantly higher than the cases where multi-step forming is used with wall angles of 76° and 80°. Likewise, for a truncated cone, the deviations are higher for the single step forming of a 60° cone than for the multi-step forming of a 80° cone. Besides, for the multi-step cases, failure occurs at the regions of high curvature in the ribs.

Table 1. Schemes of cases illustrating behavior of high wall angle features; (All parts are made with AA 3103 sheet material of 1.5 mm; negative deviations indicate over forming and positive deviation indicate under forming)

Case detail				Number of forming steps	Failure region	Failure depth	Accuracy behavior
Geometry	Wall angle	CAD model depth	Step down (mm)				
Truncated pyramid	60°	35	1	1	None	None	Min. deviation: -1.69 mm Max. deviation: 2.44 mm Mean deviation: 1.07 mm
Truncated pyramid	76°	37.5	1	3	None	None	Min. deviation: -0.21 mm Max. deviation: 0.79 mm Mean deviation: 0.29 mm
Truncated pyramid	80°	35	1	4	Semi-vertical ribs	32.5 mm	Min. deviation: -0.57 mm Max. deviation: 0.78 mm Mean deviation: 0.03 mm
Truncated cone	65°	35	1	1	None	None	Min. deviation: -1.43 mm Max. deviation: 3.14 mm

							Mean deviation: 1.30 mm
Truncated cone	80°	30	1	4	Bottom rib	30 mm	Min. deviation: 0.43 mm Max. deviation: 1.47 mm Mean deviation: 1.09 mm

Fig. 3 shows a cross-section view of a 80° truncated pyramid made in AA 3103 of 1.5 mm sheet thickness in four steps starting with a pyramid of 60° and increasing the wall angle at every step.
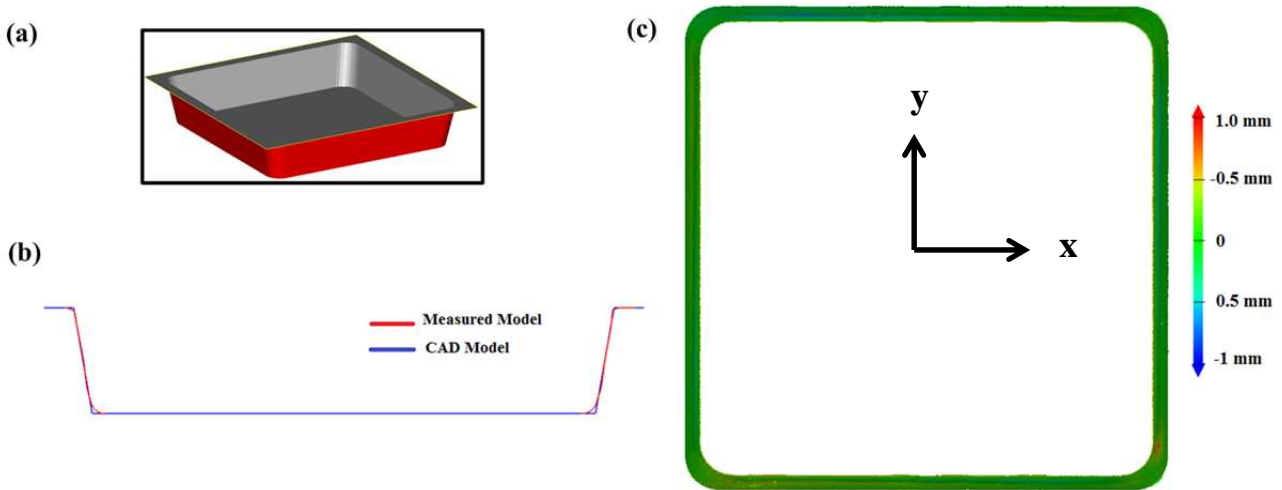
Fig.3. Truncated pyramid of wall angle 80° and depth 35 mm formed with accuracy in the range [-0.572 mm, 0.787 mm] shown in isometric view in (a), section at x=0 compared in (b) and accuracy color plot shown in (c)

It may be noted that the mild over forming effects during multi-step processing can often be very difficult to reverse, as the part is unusually bulged at these locations (Figure 4). The unusual bulging referred to here is a sudden change in the final part shape which is smooth and planar close to the top, and suddenly exhibiting an outwards dent on the surface due to the over forming.
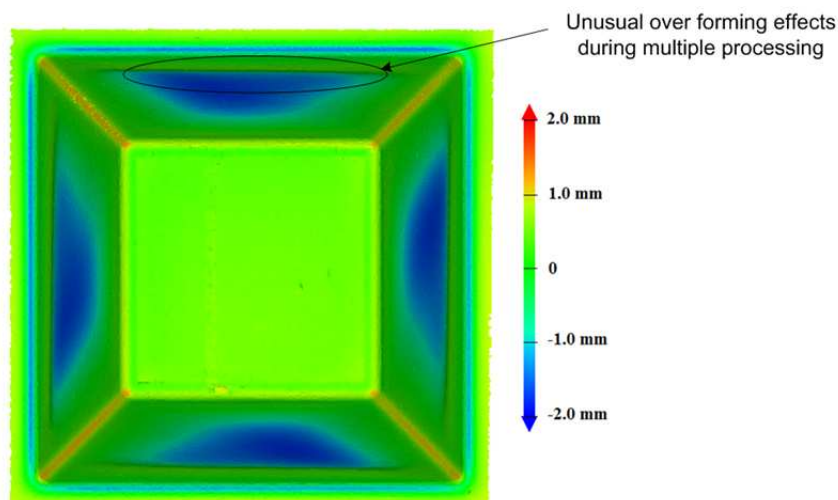
Fig.4. Effects of multiple processing on a pyramid of wall angle 70° made with AA 1050 of 1.5 mm

Interactions of high wall angle features. Feature interactions play a key role in incremental sheet forming [13, 14]. The interaction of high wall angle features with other features was found to

result in sharp dimensional inaccuracies, especially, when the features in interaction had a large difference in wall angles. A specific case of a two slope truncated pyramid of 80° (depth 35 mm) and 25° (depth 17.5 mm) made in AA 3103 of thickness 1.5 mm is illustrated in Fig.5, where the forming of the lower plane result in severe inwards buckling of the top plane which had hitherto been formed with a high accuracy as shown in Fig. 3. This results in a maximum deviation of 10.04 mm which is nearly 5 mm more than a conventional tent effect phenomenon (shown in Fig. 6), and a small crack in the final part is also observed at the location of the ribs.
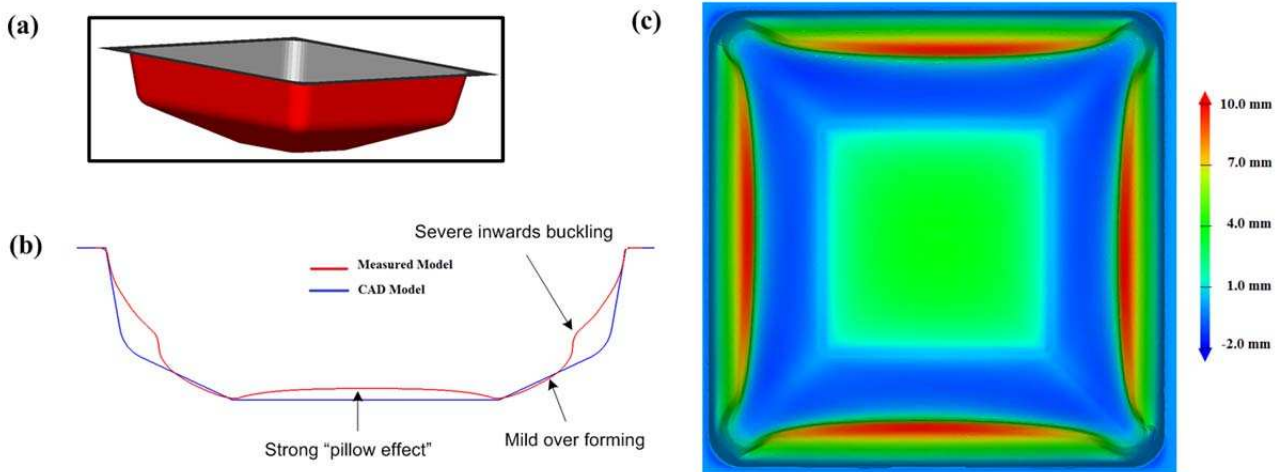
Fig.5. Two slope truncated pyramid of top plane wall angle 80° and depth 35 mm formed in combination with bottom plane with wall angle 25° and depth 17.5 mm with accuracy in the range [-1.243, 10.04 mm] shown in isometric view in (a), section at x=0 compared in (b) and accuracy color plot shown in (c)
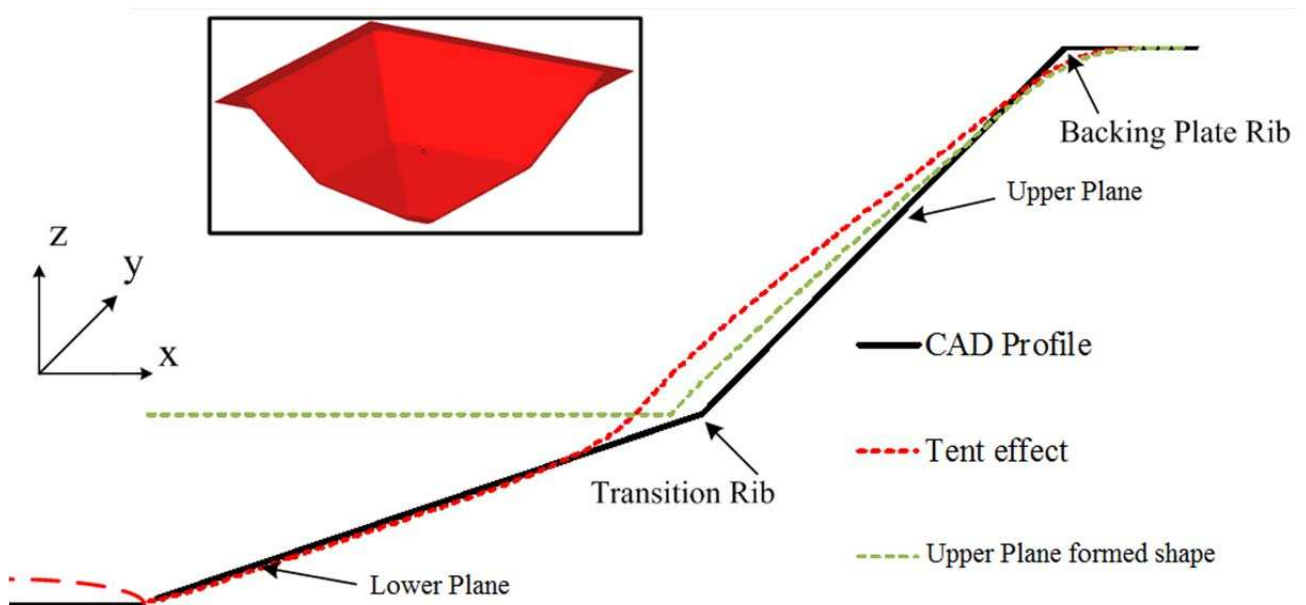
Fig.6. Conventional tent effect phenomenon illustrated for the forming of a two slope pyramid; the green dotted line shows the shape formed at the end of forming the top planar face and the red dotted line shows the shape formed at the end of forming the lower plane; the tent effect occurs as a result of pulling of the top plane by the bottom plane when the bottom plane is being formed

Offset distances between successive tool paths. The forming of high wall angle features using a succession of shapes requires that folding over of the sheet must be avoided in order to prevent failure (Fig. 7a). The test for folding over for a typical multi step path needs to be done at the bottom of the path, because the offset distances between the paths is the highest here. For two shapes of wall angles β followed by α, formed with a tool of radius R, the maximum offset distance can be evaluated from the geometrical drawing shown in Fig. 7b to be:

$$d = \frac{R}{\tan(\gamma)}, \text{ where } \gamma = \frac{180° - \alpha}{2} \tag{1}$$

(a)   (b)
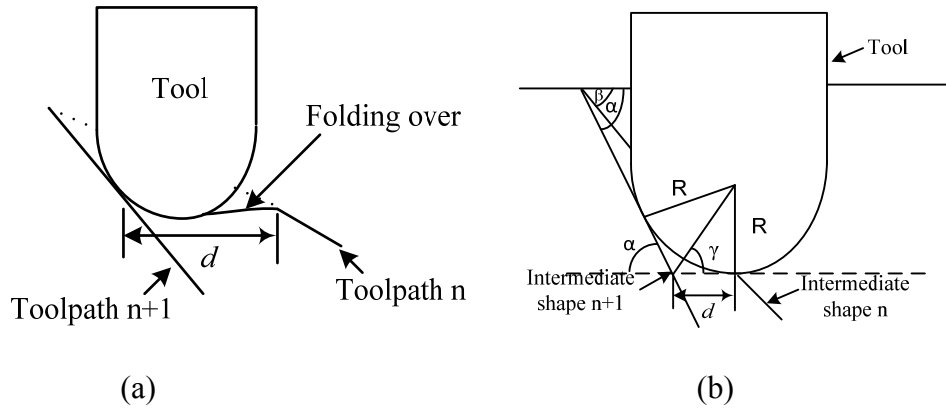
Fig.7.(a) Folding over effect at too large offset between successive tool path passes, (b) Maximum offset between successive tool paths in multi-step processing of parts

Multi-step mesh morphing

While many manufacturing processes use stepwise product shaping, morphing in particular has also been shown to be specifically useful for certain manufacturing processes such as multi-axis rough milling [15]. The basic concept in morphing is the use of a source object and a target object. In this work, the input objects are triangulated models in STL file format. As the STL format is a boundary representation (BREP) technique, the morphing problem needs to be solved in two phases: the correspondence problem and the interpolation step. Further, as different features behave differently in incremental forming, the mapping process needs to take into account feature behavior. Besides, specific SPIF based constraints need to be incorporated to complete the final model creation and tool path generation, as explained below.

Source and target objects. The correspondence problem deals with finding a suitable mapping between the source and target objects. Hence, an intelligent definition of these objects is essential to solving the next problem dealing with finding intermediate shapes using interpolation. An example of this concept for morphing images is illustrated in Fig. 8. The morphing of images is a two dimensional problem, and is often used in animation. It consists of two steps, viz.: the warping step and the cross dissolving step. In the warping step, the correspondence between the features in the source and target objects is established. The cross dissolving step creates interpolations between the pixels of the source image and the pixels of the warped images of the target image. However, the problem of three dimensional morphing is different than the two dimensional problem. In the 3D problem, a set of intermediate objects have to be generated between a source object in 3D and target object in 3D. The data sets involved in the 3D morphing problem are different and hence, requires a different approach than 2D morphing. As incremental forming deals with converting a flat blank shape into a formed shape, an inverse approach is used here, where the final part model is made the source object for morphing and the flat blank is made the target object. The source object is successively deformed to finally be a flat blank, and of the numerous intermediate shapes generated,

specific shapes are chosen depending on the offset distances between successive tool paths which are related to the wall angles in the final part and intermediate shapes.

Fig.8. Example of image morphing starting with the image of an incremental forming researcher Johan Verbert as the source and the image of one of the authors as the target showing intermediate images generated using the commercial software Morpheus Photo Morpher [16]

Feature based mesh morphing. The mesh morphing strategy is applied selectively to individual features, based on their feature behavior. A rule set has been developed for this purpose. Some of the basic rules governing the feature based morphing are listed below:

1. Planar features which do not undergo shape distortion during incremental forming, such as the horizontal top plane located at the level of the backing plate, are not morphed.
2. Planar features which are in interaction with a feature below them separated by a transition rib feature are morphed inwards together with the rib and the interacting feature, creating a smooth positive curvature intermediate shape.
3. Bottom planar features, which are expected to show a pillow effect, are also morphed along with the rest of the part into an intermediate smooth positive curvature surface, which ensures that the material is more evenly distributed during the pre-processing stages, thereby reducing the pillow effect.
4. Low wall angle and negative curvature features are morphed significantly inwards by applying more morphing steps as compared to high wall angle features, in order to reduce the final over forming. The exact number of steps is decided by the magnitude of the curvature or wall angle of the feature. Higher the curvature or lower the wall angle, more the steps that are required.
5. Rib features are blended in with the adjacent features, which helps forming sharp feature ribs in the final part. This is done by smoothing the vertices along with the neighboring feature vertices to result in a combined feature with lower curvature than the original ribs.

The execution of the above rules is done by implementing a feature based mesh deformation that carries out differential updation of vertices based on their feature using the method outlined next.

Application of Laplacian operators. The interpolation step is carried out by deformation from a source mesh to a target mesh with the help of special Laplacian operators. Local smoothing at a vertex is carried out using the mean of positions of adjacent points, using the below operator [17]:

$$L(v_k) = \sum_{l \in k^n} w_{kl}(v_l - v_k) \tag{2}$$

Here, k^n is a vertex index corresponding to the set of neighboring vertices of v_k (see Fig. 9 for an illustration of neighborhood vertices), and w_{kl} is a weight for the edge (k,l) with $\sum_{l \in k^n} w_{kl} = 1$. In order to ensure that the resulting mesh is smooth, we need to ensure the condition: $\sum_{l \in k^n} w_{kl}(v_l - v_k) = 0$. This condition can be further written in matrix form as below:

$$\mathbf{LX} = \mathbf{0} \tag{3}$$

where, $\mathbf{L}$ is an $n \times n$ matrix with elements given by:

$$L_{kl} = \begin{cases} 1 & if\ k = l \\ -w_{kl} & if\ (k,l)\ is\ an\ edge \\ 0 & otherwise \end{cases} \tag{4}$$

and $\mathbf{X}$ is an $n \times 1$ vector of vertices in the mesh.
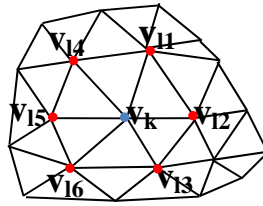
Fig.9. Illustration of neighborhood vertices v_{l1}, v_{l2}, v_{l3}, v_{l4}, v_{l5}, v_{l6} of a vertex v_k

Points within a feature can be selectively translated by using an augmented linear system with feature constraints as below:

$$\mathbf{CX^f} = \begin{pmatrix} \mathbf{L} \\ \mathbf{F} \end{pmatrix} \mathbf{X^f} = \begin{pmatrix} \mathbf{0} \\ \mathbf{d^F} \end{pmatrix} = \mathbf{d} \tag{5}$$

where, $\mathbf{F}$ is a $p \times n$ feature based constraining matrix used to create a combined matrix $\mathbf{C}$ with elements of $\mathbf{F}$ given by:

$$f_{jk} = \begin{cases} \chi & if\ k\ belongs\ to\ a\ feature\ being\ constrained \\ 0 & otherwise \end{cases} \quad 1 \le j \le p,\ 1 \le k \le n \tag{6}$$

where χ is the weight of the constraints for the vertices belonging to the feature being constrained. $\mathbf{d^F}$ is a $p \times 1$ column vector with elements given by the product of the feature vertex weights and the vertex co-ordinates. It may be noted that the vector $\mathbf{X}$ in (3) and the vector $\mathbf{X^f}$ in (5) are not the same size vectors. The second vector has the physical interpretation as that of application of tunable constraints based on the feature type and incorporating knowledge of the feature behavior as observed in incremental sheet forming. In Fig. 10, an illustration of features that may be constrained and features that may not be constrained is shown. An example of a feature that may not be constrained is the horizontal top planar feature at the level of the backing plate, while an example of a feature that is constrained is the non horizontal planar feature.

The feature constrained vertices can now be obtained as:

$$\mathbf{X^f} = (\mathbf{C^T C})^{-1} \mathbf{C^T d} \tag{7}$$
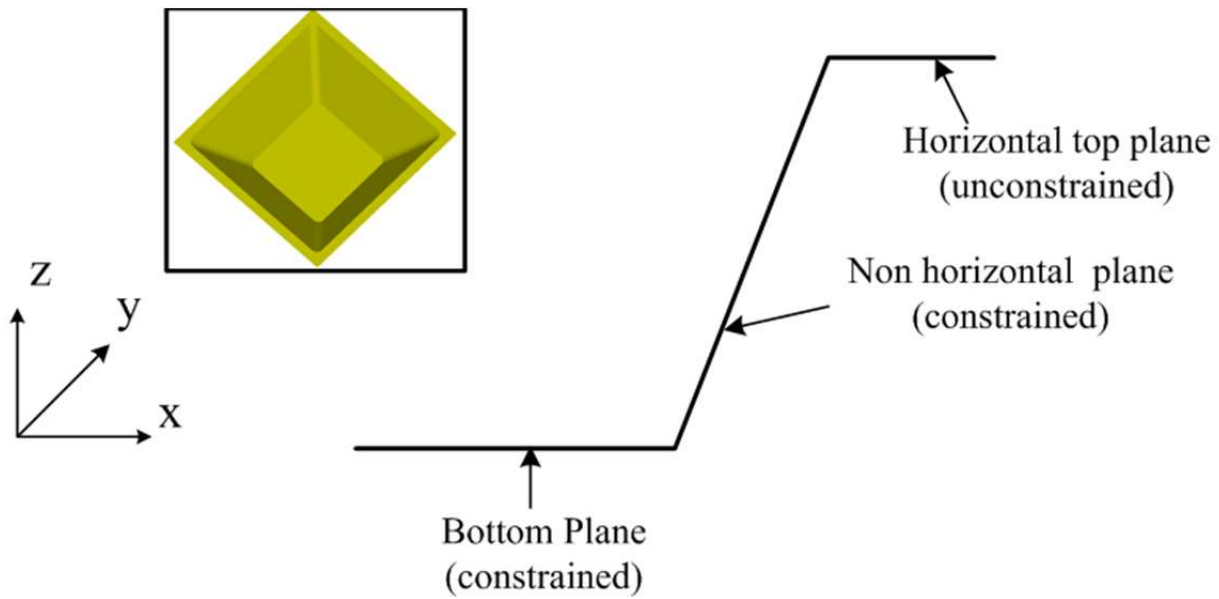
Fig.10. Constraining different features – the top plane is left unconstrained as it does not deform, while the non horizontal and bottom planes are deformed as they show deviations which can be improved upon using morphing

The Laplacian operators are used because the final target mesh is a flat blank and by the application of this technique, the final target geometry can be achieved while avoiding the possibility of a distorted intermediate geometry. The implementation of the morphing steps is done within the software MeshLab [18]. The result of the mesh morphing technique for a human face is shown in Fig. 11. The number of required morphing meshes is discussed in the next section.
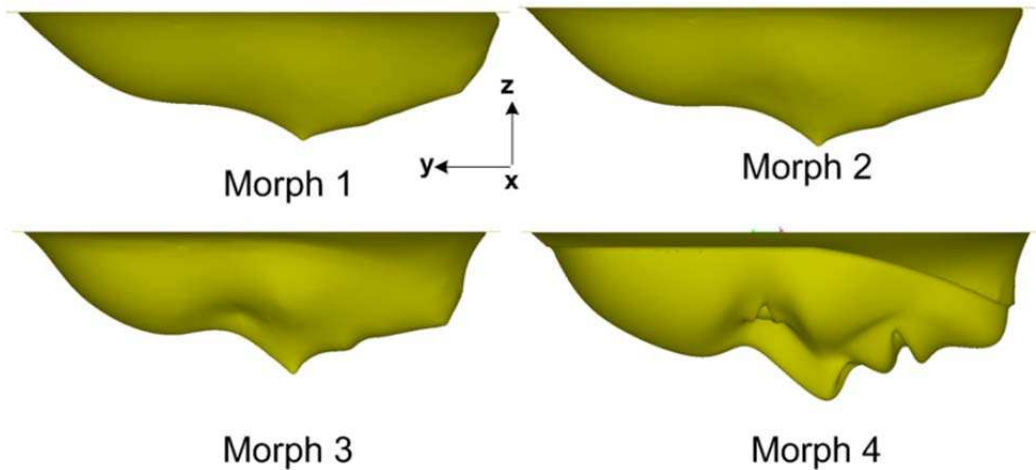
Fig.11. Example of mesh morphing where a human face (Morph 4) is morphed to a ruled surface (Morph 1) and finally to a flat blank

Incorporating SPIF process constraints. After application of the above transformation to the source matrix for a certain number of iterations of application of Equations (2)-(7), a number of intermediate meshes are obtained. The number of iterations is dependent on the part size and geometrical features in the part which are defined within the process planning system, so as to generate meshes which are sufficiently distinct from each other. However, as the morphed meshes

are developed on specific features, especially excluding the top horizontal plane, the meshes needs to be adapted for incremental forming and also the suitable morphed meshes need to be selected. This is done in three steps: i) using a Bezier curve based extension to the backing plate, as illustrated in Fig. 12, ii) remeshing and iii) mesh selection by checking the criterion given in Equation (1).
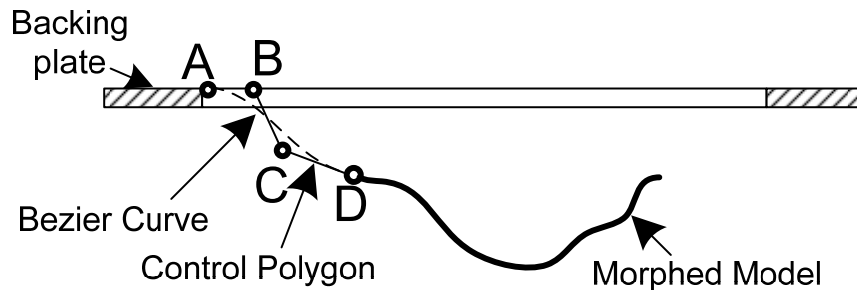
Fig.12. Extension of morphed model to backing plate

The use of a spline based extension is essential to maintain C^1 continuity in the transition from the backing plate to the morphed model. For every point D on the boundary of the morphed model, a corresponding point A is located on the backing plate model. The intermediate points on the control polygon, B and C, are selected so that the resulting curve is C^1 continuous. The curve shape can be controlled by the length of the segments $\vec{AB}$ and $\vec{CD}$. The extension step is followed by a remeshing step which is needed in order to refine the mesh for subsequent tool path generation using partial tool paths. Since the morphing procedure can generate an infinite number of intermediate shapes that lead up to the target mesh, a mesh selection criterion is used based on Equation 1. Two important considerations are kept in mind here. First, the wall angles in the final part decide how many intermediate shapes need to be used. For instance, if the final part has a maximum wall angle of 80° and a failure wall angle of 76°, it is useful to start with an intermediate shape which has a wall angle of 50° (set as 2/3rd of the failure angle as a thumb rule), chosen based on the forming limit for the material. Secondly, the offset between the intermediate shapes is checked to see that it is not greater than the distance in (1).

Intelligent sequencing of tool paths

The use of morphed surfaces is not always sufficient to obtain parts with high accuracy. In addition, the tool paths for individual features need to be combined in a sequential manner to achieve the desired accuracy. The different challenges in sequencing tool paths, algorithms for sequencing and results of sequencing are presented below.

Sequencing challenges. Using a feature based slicing algorithm, tool paths for individual features are generated, as shown in Fig 13. These tool paths then need to be sequenced and combined to generate continuous tool paths that conform to the SPIF process. However, this sequencing effort comes with a few challenges. First of all, the tool paths for individual features are curves or polylines ordered with increasing depth. So, the curves for each tool path at a specific depth need to be brought together. Next, at a specific depth, they need to be arranged sequentially, maintaining directionality. Then, the step down from one depth to the next may have points located at a different spatial location than the end of the contour, resulting in cris-crossing across the part. This needs to be avoided. Further, the tool path needs to be initiated from a safe tool position relative to the part in the beginning and retract out at the end. Fig. 14 shows the challenges involved in sequencing.
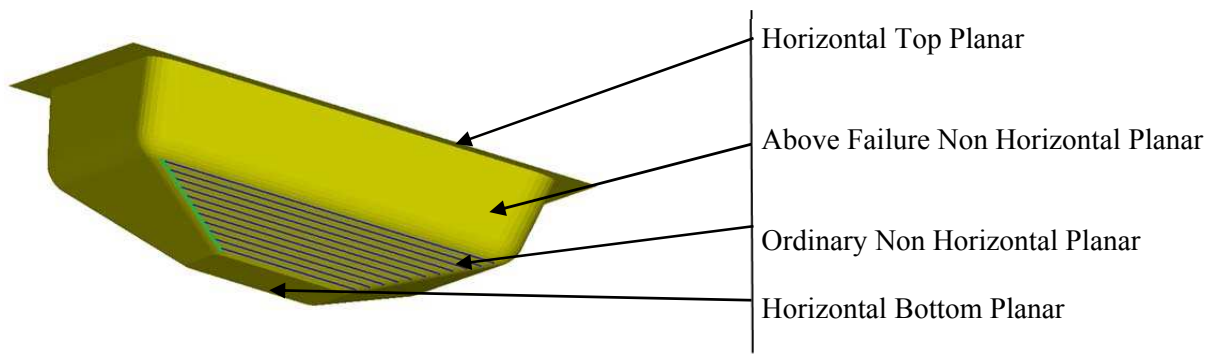
Fig.13. Example of a feature specific partial tool path made on the ordinary non horizontal planar feature

Sequencing algorithms. The sequencing procedure is carried out in three steps. First, the different tool paths available as separate CNC G-code files are integrated into a single tool path model. Here, it may be noted that these G-code files can be obtained from different toolpath models, using post-processing functions available within the in-house software for incremental sheet forming, FSPIF, which were developed in the research done by Verbert [7]. The post-processing functions enable generation of toolpaths compatible to different machines using in the incremental sheet forming research such as MAHO 600C, Aciera F45, EDM Robofil 2000 and KUKA KR210. Next, the tool paths at a specific depth are grouped together, so as to arrange all the tool path curves by depth (Algorithm 1 in Appendix A). These curves are then subjected in the third step to a XY-sequencer, which uses the polar co-ordinates of the points on the curves to arrange them in a specific direction without intersections (Algorithm 2 in Appendix B). In addition, the additional step down points in the z-direction are eliminated and the step down locations are placed where the curve in the previous contour is closed. Both algorithms are detailed in the Appendix.

The integrated tool path generation for the full part is done by keeping in mind the topology of the part, by following the below rules:

1. For complex parts, often different features may have different wall angle variations. For instance, if we consider a part which has a positive general horizontal ruled (PGHR) surface connected to a negative general horizontal ruled (NGHR) surface by the relation "is 2nd horizontal neighbor of" between the depths z=0 (at the level of the backing plate) and z=-30 mm (bottom of the part). In this case, the PGHR surface will have wall angles that start with a high value at z=0 and decrease to nearly zero degrees at z=-30 mm. In contrast, the NGHR surface will have a lower value at z=0 and increase to a high value at z=-30 mm. With a constant step down of 0.5 mm, the tool paths at the top for the NGHR part will have very high scallop distances, while the tool paths for the PGHR part will have very high scallop distances at the bottom. Hence, for such cases, a well-chosen scallop distance is used for the entire part to generate the tool path instead of a constant step down.
2. The tool paths are first sequenced by depth, i.e. z-axis co-ordinates using a sort function.
3. Next, at a specific depth, they are arranged in order of neighborhood of the features in the horizontal direction.
4. The vertices in the polylines formed by the tool paths at a specific depth are sorted using the polar co-ordinates of the points so that uni-directionality is maintained.
5. Wherever necessary, the tool is made to retreat in the z-axis direction by a specific distance determined by the part geometry, and plunge back in at the right co-ordinates. This is especially necessary for processing only individual features, or while moving from one feature to another that is not a neighbor of the preceding feature. Further, this step may be necessitated to avoid collisions between the tool and the part, depending on the geometry.
6. Vertical z-axis step downs are introduced when the tool moves from one depth to another.

Sequencing results. The sequencing algorithms were tested on a tool path for a truncated pyramid with four planar faces separated by semi-vertical ribs. Fig 14 (e) shows the result of the sequencing for the first three contours. The algorithms worked well for a number of test cases illustrated below.
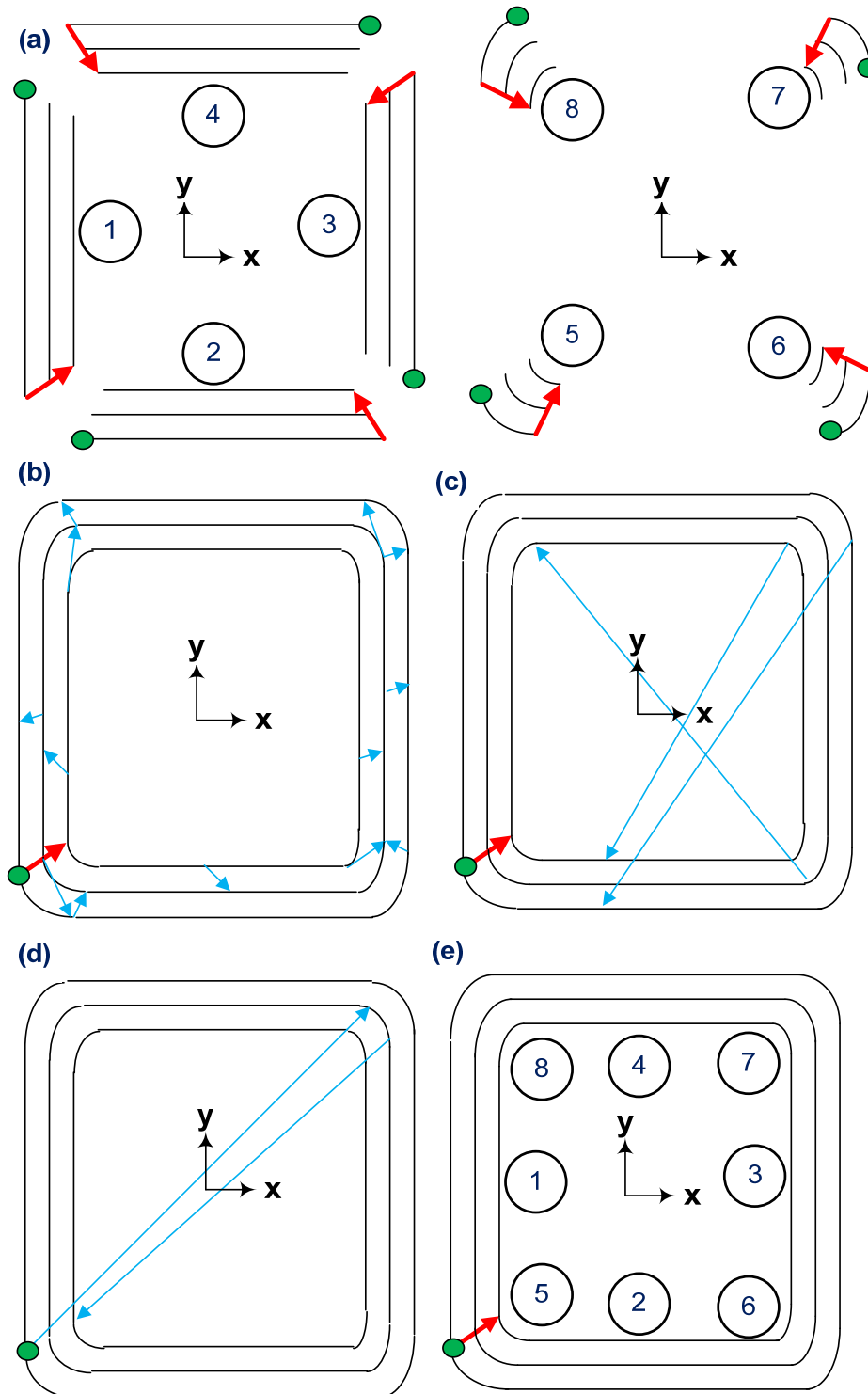
Fig.14. Sequencing of tool paths showing (a) feature tool paths for planar features (1-4) and ribs (5-8) (b) tool axis sequencing errors (c) xy-plane sequencing errors (d) step down sequencing errors (e) correctly sequenced tool paths (*errors are shown with blue lines; the direction of arrows indicates the directionality of the tool path in the z-axis; the green circles indicate the start points of the tool paths*)

Case studies

Pyramid manufacture.

A truncated two slope pyramid with top planar face wall angle 80° (depth 35 mm) and bottom planar face (depth 25 mm) wall angle 25° was formed in AA 1050 sheets (forming limit of 76°) of 1.5 mm thickness using an integrated procedure of generating morphed surfaces and integration of partial tool paths for individual features. The morphed surfaces used for the manufacture are illustrated in Fig. 15. A cylindrical stylus with hemi-spherical end of diameter 10 mm was used for the forming process with oil based lubricant on a 3-axis milling machine. The accuracy plot for the part is shown in Fig. 16(a).
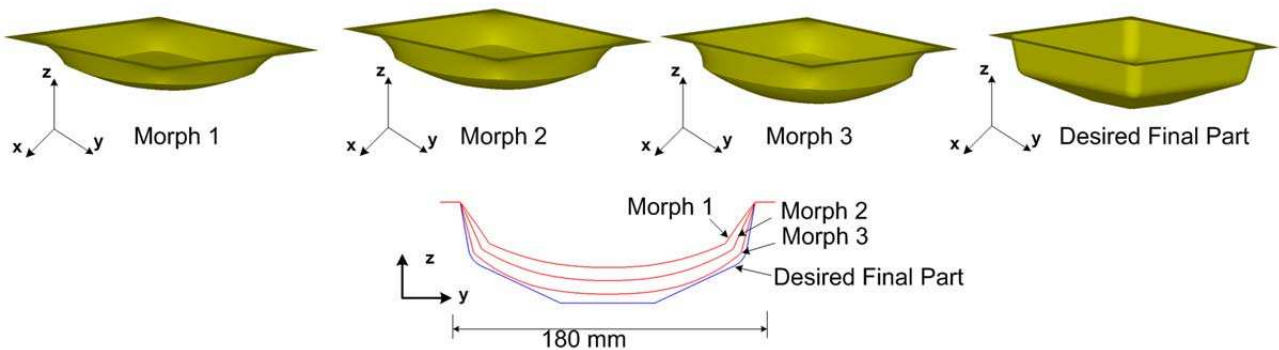
Fig.15. The final part, an above failure limit truncated two slope pyramid with wall angles 80° and 25°, is used as the source object for generating the morphed surfaces in the order Morph 3→Morph 2→Morph 1 using the vertex transformation in Equation (7) and extension to the backing plate.

In a second case, a truncated two slope pyramid with wall angles well below failure (wall angles of 60° and 30° with depths 60 mm and 30 mm respectively) was formed with AA 1050 sheets of 1.5 mm thickness using a similar procedure. The accuracy plot for the part made with the morphed tool path generation strategy is shown in Fig. 16(b). Table 2 lists the accuracies of the formed parts.

(a)　　　　　　　　　　　　　　　　　　(b)
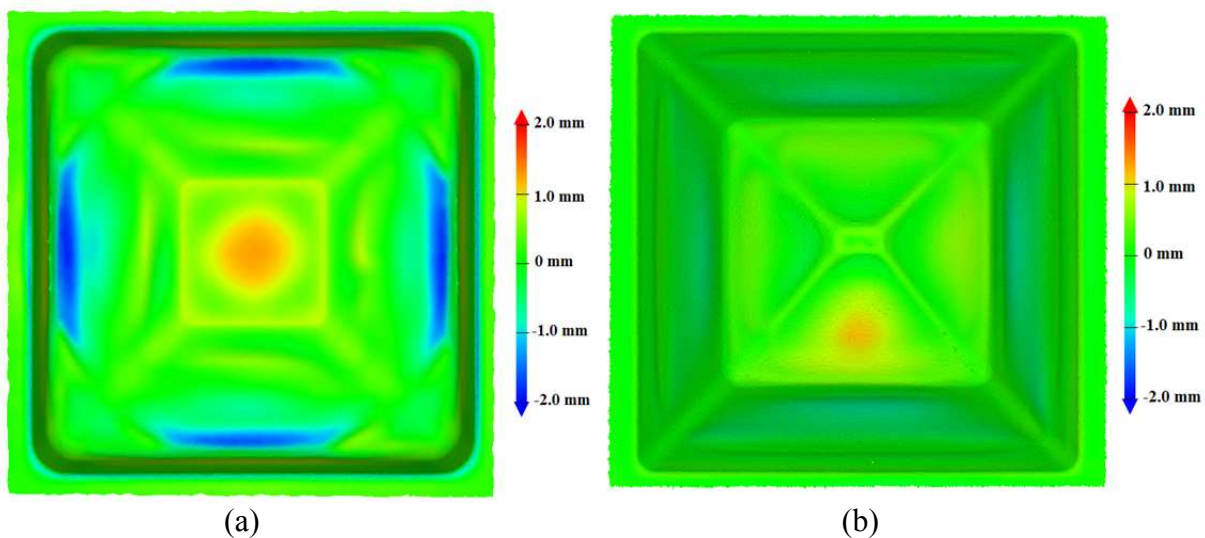
Fig.16. Accuracy plots of truncated pyramids made with morphed tool paths in combination with intelligent sequencing of tool paths for (a) pyramid with wall angles 80° and 25° (b) pyramid with wall angles 60° and 30°

A comparision of the pyramid formed by the classical multi-step approach, as shown in Fig. 5 and the same geometry with wall angles of 80° and 25° formed by using the multi-step forming approach shows that the maximum deviations are significantly reduced from more than 10 mm to less than 1 mm using the morphing technique (see Table 2). Moreover, in the traditional multi-step approach, the part showed failure close to the ribs, which was absent in the morphing approach.

Airfoil manufacture.

To illustrate the capabilities of the integrated tool path generation technique system in systematic part manufacture, airfoil manufacture using stainless steel grade AISI 304 of 0.5 mm thickness was undertaken. Fig. 17 shows the original airfoil whose CAD model available freely on GrabCAD by Mark Drela was used for the part manufacture [19]. This airfoil is designed for low Reynolds number, laminar flows. A view of the CAD model is also shown here alongwith a section view. The dimensions of the original airfoil are: 48 m x 9.991 m. A 0.3 % scaled model of size 144 mm x 29.973 mm was selected for manufacture.
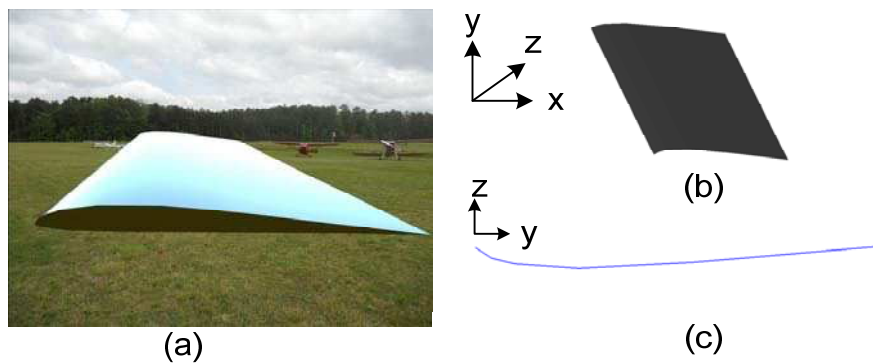
Fig.17. Airfoil design (a) picture of original model of airfoil [19] (b) STL model of the airfoil (c) cross-section of the airfoil taken at X=0 in the co-ordinate system shown for (b)

The manufacture of the airfoil was done using the following steps:

1. **Extension of the part to the backing plate.** The part was extended to the backing plate using a planar hole filling algorithm within the software Magics provided by Materialise [20]. The planar extension was chosen so that the airfoil can be easily identified in the formed part. Fig. 18 shows the extended part geometry, dimensions and section views.
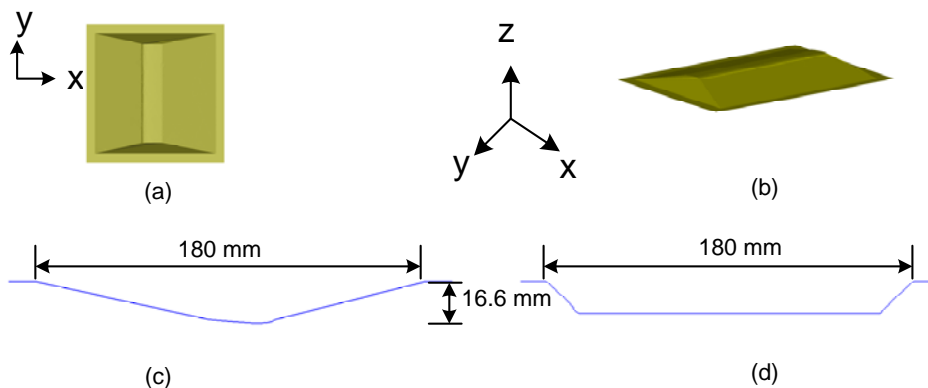
Fig.18. Extended airfoil model for manufacture showing (a) top view in xy plane (b) isometric side view (c) sectional view at X=0 (d) sectional view at Y=0

2. **Model compensation and toolpath generation.** A morphed surface was generated using the morphing technique illustrated in the earlier sections. Toolpaths were generated with a small step down of 0.25 mm, to account for the low wall angle features in the part.

To illustrate the advantages of the morphing approach, two types of parts were made: i) parts made using tool paths generated directly on the CAD model of the airfoil or uncompensated and ii) morphed parts on a 3-axis milling machine. A cylindrical tool with a hemispherical ball end of diameter 10 mm was used at a feed rate of 2 m/min. The tool rotation speed was set to approximate rolling contact, and an oil based lubricant was used. Fig. 19 shows the colors plots of accuracy and pictures of the manufactured parts. The results show that the maximum deviation with an uncompensated toolpath is 2.195 mm, while with the integrated morphing and sequencing strategy, it is 0.497 mm. The average positive deviation also improves with the compensated toolpath and is seen at ~ 0.3 mm.
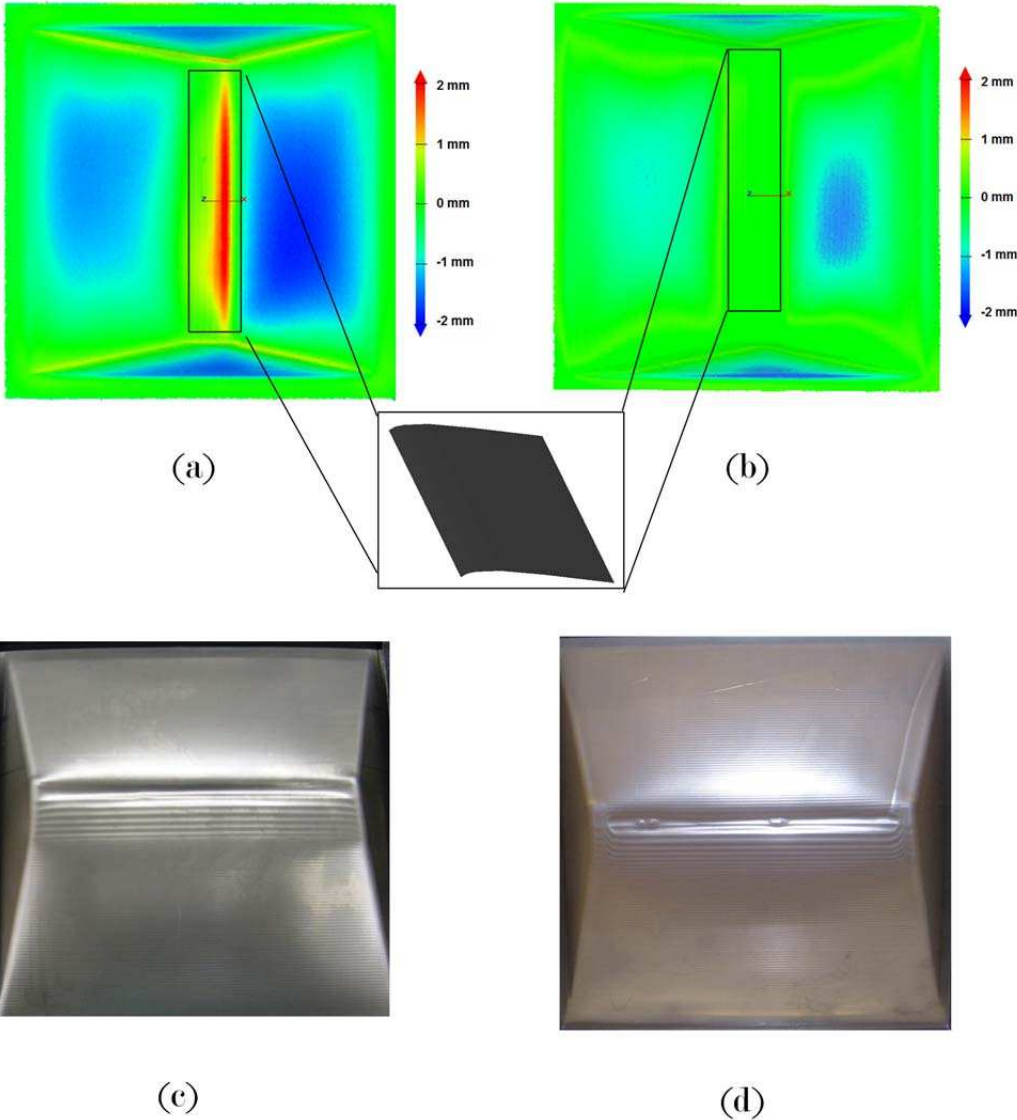
Fig.19. Airfoil manufacture and accuracy results showing: (a)-(b) color plots of accuracy for (a) AISI 304 part made with uncompensated toolpath (d) AISI 304 part made with a morphed surface; rectangular inset in each color plot shows the section of the airfoil (c)-(d) shows the actual manufactured parts made with (c) AISI 304 uncompensated (d) AISI 304 made with the integrated morphing strategy

Table 2. Accuracies of formed parts *(All dimensions are in mm, the pyramids are formed using the integrated morphing strategy)*

Part	Average Positive Deviation	Average Negative Deviation	Maximum Deviation	Minimum Deviation	Average Deviation	Standard Deviation
Pyramid Top 80 Bottom 25	0.324	-0.484	0.999	-1.754	0.069	0.469
Pyramid Top 60 Bottom 30	0.299	-0.345	0.989	-1.178	-0.025	0.422
Airfoil Uncompensated	0.715	-0.150	2.195	-0.624	0.625	0.572
Airfoil Integrated Morphing	0.317	-0.321	0.497	-0.767	0.001	0.274

Conclusions

A systematic method for creating multi-resolution morphed surfaces for incremental sheet forming has been outlined. The technique for morphing starts with a source object, which is the same as the final part that has to be formed. Starting with this source object, intermediate geometries can be generated by using a Laplacian operator, and incorporating additional incremental forming constraints. These intermediate geometries help in the manufacture of parts with wall angles above the failure limit of the material being formed. Further, they substantially reduce the effect of interactions with other features within the part.

In addition to multi-step morphing, proper sequencing and integration of tool paths is essential to enable accurate part manufacture. Algorithms that enable sequencing and integration of feature specific partial tool paths were discussed in this paper. The integrated morphing technique and tool path generation algorithms can now be integrated within a process planning system, such as the one described in [21] and can be used in combination with advanced feature detection algorithms [22].

The use of the integrated technique allows the manufacture of high forming angle parts with improved accuracy. It was shown that for a two slope pyramid with top plane wall angle of 80°, the maximum deviation using the integrated technique was less than 1 mm, while without the use of this method the maximum deviation was more than 10 mm. Likewise, for an airfoil shape made in stainless steel, while the maximum deviation was more than 2 mm with an uncompensated tool path, the maximum deviation with the integrated morphing strategy is less than 0.5 mm. This technique also helps prevent failure especially in regions with high curvature such as ribs and enables automated generation of intermediate shapes for multi-step processing using incremental sheet forming. This integrated technique can be extended to freeform surfaces as well, thereby enabling manufacture of complex 3D shapes in the future.

Acknowledgements

References

[1] Jeswiet J, Micari F, Hirt G, Bramley A, Duflou J, Allwood J (2005) Asymmetric single point incremental forming of sheet metal. CIRP Annals-Manufacturing Technology 54:623-649.

[2] Hagan E, Jeswiet J (2003) A review of conventional and modern single-point sheet metal forming methods. Proceedings of the Institution of Mechanical Engineers Part B-Journal of Engineering Manufacture 217:213-225.

[3] Meier H, Smukala V, Dewald O, Zhang J (2007) Two Point Incremental Forming with Two Moving Forming Tools. Key Engineering Materials Volume 344:599-605

[4] Franzen V, Kwiatkowski L, Martins PAF, Tekkaya AE (2009) Single Point Incremental Forming of PVC. Journal of Materials Processing Technology 209(1):462-469

[5] Martins PAF, Kwiatkowski L, Franzen V, Tekkaya AE, Kleiner M (2009) Single Point Incremental Forming of Polymers. CIRP Annals - Manufacturing Technology 58(1):229-232

[6] Behera AK, Verbert J, Lauwers B, Duflou JR (2012) Tool path compensation strategies for single point incremental sheet forming using multivariate adaptive regression splines. Computer-Aided Design 45:575-590

[7] Verbert J, Duflou J, Lauwers B (2007) Feature based approach for increasing the accuracy of the SPIF process. Key Engineering Materials Vol. 344:527-534

[8] Bambach M, Araghi BT, Hirt G (2009) Strategies to improve the geometric accuracy in asymmetric single point incremental forming. Prod. Eng. Res. Devel. 3:145-156

[9] Ambrogio G, Costantino I, De Napolia L, Filice L, Fratini L, Muzzupappa M (2004) Influence of some relevant process parameters on the dimensional accuracy in incremental forming: a numerical and experimental investigation. Journal of Materials Processing Technology, 153-154:501-507

[10] Duflou J, Verbert J, Belkassem B, Gu J, Sol H, Henrard C, Habraken AM (2008) Process window enhancement for single point incremental forming through multi-step toolpaths. CIRP Annals - Manufacturing Technology, 57(1):253-256

[11] Duflou J, Callebaut B, Verbert J, De Baerdemaeker H (2008) Improved SPIF performance through dynamic local heating. International Journal of Machine Tools and Manufacture 48(5):543-549

[12] Skjødt M, Bay N, Endelt B, Ingarao G (2008) Multi stage strategies for single point incremental forming of a cup. International Journal of Material Forming 1:1199-1202.

[13] Behera AK, Vanhove H, Lauwers B, Duflou JR (2011) Accuracy improvement in single point incremental forming through systematic study of feature interactions. Key Engineering Materials 473:881-888

[14] Behera AK (2013) Shape Feature Taxonomy Development for Toolpath Optimisation in Incremental Sheet Forming. PhD Dissertation, Katholieke Universiteit Leuven

[15] Lefebvre P, Lauwers B (2005) 3D morphing for generating intermediate roughing levels in multi-axis machining. Computer-Aided Design & Applications 2(1-4):115-123

[16] Morpheus Photo Morpher (2013) www.morpheussoftware.net Accessed 23rd December, 2013

[17] Ji Z, Liu L, Wang G (2005) A global laplacian smoothing approach with feature preservation. Proceedings of the 9th Intl. Conf. on Comp. Aided Design and Computer Graphics 269-274

[18] MeshLab (2013) http://meshlab.sourceforge.net Last accessed 20th July 2013.

[19] Drela M (2013) AG-45C-03F Airfoil. GrabCAD. http://grabcad.com/library/mark-drela-ag-45c-03f-airfoil-1. Accessed 18th June 2013.

[20] Materialise NV (2012) Magics, the most powerful STL editor – Software for additive manufacturing. http://software.materialise.com/magics Accessed 20th July 2013.

[21] Behera, A., Lauwers, B., Duflou, J. (2014). Tool Path Generation Framework for Accurate Manufacture of Complex 3D Sheet Metal Parts using Single Point Incremental Forming. Computers in Industry, Available online 4 February 2014, http://dx.doi.org/10.1016/j.compind.2014.01.002.

[22] Behera, A., Lauwers, B., Duflou, J. (2012). Advanced Feature Detection Algorithms for Incrementally Formed Sheet Metal Parts. *Transactions of Nonferrous Metals Society of China.* 22 (Special 2), s315-s322

Appendix A

Algorithm 1: *Algorithm for sequencing in tool axis*

Input: Tool paths for individual features, T_1, T_2, … T_N
Output: Integrated tool path T_{iz} sequenced in tool axis direction 'Z'

For each (ToolPathModel T_K in ToolPathList { **T_1, T_2, … T_N**})
{
      For each curve C in T_K {
          Add C to ToolPathModel T_{int}
      }
}
Create a new point list **L_{poly}**
For each curve C in T_{int} {
For each (Point p in C) {
         Add p to **L_{poly}**
      }
}
Sort **L_{poly}** by Z-Coordinate
For each (Point p in **L_{poly}**) {
         Add p to T_{iz}
}

Appendix B

Algorithm 2: *Algorithm for sequencing in XY plane*

Input: Tool path T_{iz} sequenced in tool axis
Output: Tool path T_{xy} sequenced in xy-plane

Create a new curve **prevcurv**
For each curve C in T_{iz} {
Create a new polyline **newpoly**
Create a new point list **S_{poly}**
if ((C.Start.ZCoord > 0) && (C.End.ZCoord <= 0)) {
prevcurv = C
// Identified as initial plunge; Curve not added as initial plunge is determined after XY sequencing of first contour
}
else if ((curv.Start.ZCoord > 0) && (C.End.ZCoord > 0)) {
Add C to ToolPathModel T_{temp}

// This is an intermediate plunge outside the work piece definitions and does not result in any tool path intersections and can thus be simply added to the curve list
prevcurv = C
}
else if ((C.Start.ZCoord <= 0) && (Math.Abs(C.Start.ZCoord - C.End.ZCoord) > stepdownthreshold)) {
// Identified as a stepdown; Curve not added to avoid step down errors
}
else if ((C.Start.ZCoord <= 0) && (Math.Abs(C.Start.ZCoord - C.End.ZCoord) <= stepdownthreshold)) {
// Identified as contours at the same depth
if (**prevcurv** != null) {
          if ((Math.Abs(curv.Start.ZCoord - **prevcurv**.Start.ZCoord) > stepdownthreshold))
        {
        // Current contour is at different depth than the previous contour
        For each (Point pl in C) {
            Add pl to S_{poly}
        }
        Sort S_{poly} by polar angle of points given by Atan2((Y-Coordinate-Y-Center)/(X-Coordinate-X-Center))
        // (XCenter, YCenter) is the workpiece center co-ordinates typically (0,0)
        For each (Point plp in S_{poly}) {
            Add plp to **newpoly**
        }
        Add **newpoly** to ToolPathModel T$_{temp}$
        prevcurv = **newpoly**
        }
      else if ((Math.Abs(C.Start.ZCoord - **prevcurv**.Start.ZCoord) <= stepdownthreshold))
        {
        // Current contour is at same depth as the previous contour
        Remove **prevcurv** from ToolPathModel T$_{temp}$
        For each (Point plp in **prevcurv**)
        {
            Add plp to S_{poly}
        }
        For each (Point cplp in C)
        {
            Add cplp to S_{poly}
        }
        Sort S_{poly} by polar angle of points given by Atan2((Y-Coordinate-Y-Center)/(X-Coordinate-X-Center))
        For each (Point plp in S_{poly}) {
            Add plp to **newpoly**
        }
        Add **newpoly** to ToolPathModel T$_{temp}$
        prevcurv = **newpoly**
        }
}
else if (**prevcurv** == null) {
          For each (Point pl in C) {
              Add pl to S_{poly}
          }

Sort **S**_{poly} by polar angle of points given by Atan2((Y-Coordinate-Y-Center)/(X-Coordinate-X-Center))

```
            Sort Spoly by polar angle of points given by Atan2((Y-Coordinate-Y-
      Center)/(X-Coordinate-X-Center))
      // (XCenter, YCenter) is the workpiece center co-ordinates typically (0,0)
      For each (Point plp in Spoly) {
            Add plp to newpoly
      }
      Add newpoly to ToolPathModel Ttemp
      prevcurv = newpoly
}}}
For each (Curve curv in Ttemp) {
      if((curv.Length>0)||(curv.End.ZCoord>0)) {
            Add curv to ToolPathModel Txy
   }
}
```

Appendix C

Some guidelines on the use of the feature based morphing technique using the Laplacian approach given by Equations (2)-(7) are discussed here.

- It was observed that when the weights given by χ are low (typically $\chi < 3$), then the points in the smoothed mesh are far away from the detected feature points in the mesh, while when they are high, the points are closer to the feature points.

- The matrix $\mathbf{C^T C}$ is a sparse matrix as the only non-zero entries in every row are the neighborhood are the vertices in the neighborhood. A sparse linear system needs to be solved. This can be done by finding the Cholesky factorization of the matrix $\mathbf{C^T C}$ given as $\mathbf{R^T R}$. Next, two triangular linear systems are solved to solve $\mathbf{R^T R X = C^T b}$. These are $\mathbf{R^T X^*} = \mathbf{C^T b}$ and $\mathbf{R X = X^*}$.